

Exchange instabilities in electron systems: Bloch versus Stoner Ferromagnetism

Ying Zhang and S. Das Sarma

*Condensed Matter Theory Center, Department of Physics,
University of Maryland, College Park, MD 20742-4111*

(Dated: December 2, 2024)

We show that 2D and 3D electron systems with the long-range Coulomb electron-electron interaction could develop ferromagnetic instabilities due to strong exchange effects at low densities. The critical densities in both 2D and 3D systems at which the magnetic instability, which could either be of Stoner type (second-order) or of Bloch type (first-order), are higher than the dispersion instability critical density where effective mass at the Fermi surface diverges. We discuss the theoretical as well as experimental implications of the ferromagnetic instability at low electron densities, particularly in low-disorder semiconductor-based two-dimensional systems.

PACS numbers: 71.10.-w; 71.10.Ca; 73.20.Mf; 73.40.-c

I. INTRODUCTION

Despite extensive theoretical and experimental studies on two- and three-dimensional electron systems, the physics of these fundamental many-body systems is still far from well understood. Outstanding problems such as the nature of the 2D metal-insulator transition and the nature of ground state symmetry of electron systems continue to attract considerable attention. Especially, with the development of high mobility semiconductor based 2D electron systems such as Si MOSFETs and GaAs HGFETs, where extremely low carrier densities and very high quality can be achieved, a number of recent experiments has been carried out to measure fundamental physical quantities such as magnetic susceptibility^{1,2,3,4,5,6,7,8,9,10,11,12,13} and effective mass¹⁴ in low density 2D electron systems at low temperatures ($\lesssim 100mK$). One purpose of these studies is to obtain the ground state phase diagram for 2D and 3D electron systems with long-range Coulomb interaction. It is well known that the zero temperature 2D and 3D electron systems can be characterized by a single dimensionless interaction parameter $r_s = E_{e-e}/E_K$ (where E_{e-e} denotes the interaction energy and E_K the kinetic energy), which depends only on the density (n) of the system with $r_s \propto n^{-1/2}$ ($n^{-1/3}$) in 2D (3D) systems. For small r_s , we know that both 2D and 3D electron systems can be well described by Landau's Fermi liquid theory, where a one-to-one low energy correspondence between the non-interacting Fermi gas and the interacting Fermi liquid with weakly interacting quasiparticles behaving similar to free electrons is assured. (Actually, there is an exception even to this as at exceptionally low temperatures an interacting Fermi liquid undergoes a Khon-Luttinger superconducting transition, which we ignore for our purpose since it is of no physical relevance.) In the limit of large r_s , the system tends to reduce its interaction energy E_{e-e} at the cost of higher kinetic energy by forming into an electron crystal (the so called Wigner crystal¹⁵), which has been established by Monte Carlo studies in both 2D)¹⁶ (where the crystallization transition happens at $r_s \sim 35 - 40$) and 3D systems¹⁷ (where the transi-

tion happens at $r_s \sim 55 - 75$). How the system behaves in between the above mentioned two limits of r_s (i.e. $r_s \ll 1$ and $r_s \gg 1$) is not yet clear. It has been widely accepted, and also suggested by Monte Carlo studies, that there may exist a ferromagnetic phase in the intermediate r_s region (with $r_s \sim 25 - 35$ for 2D¹⁸ and $r_s \sim 20 - 40$ for 3D systems¹⁷). Many other theoretical studies for such high r_s value region typically start with a more or less arbitrary assumption of a particular ground state symmetry of the system. Among the various model of exotic interaction-driven electronic ground states, charge or spin density wave states, various superconducting states, glassy or clustered ground states have been much discussed in the literature.

It is important to study the evolution of the Fermi liquid state starting from the weakly interacting small r_s regime. As r_s increases, all the single particle properties of the system are increasingly renormalized by interaction effects. The question is whether the Coulomb interaction renormalization brings about certain instabilities eventually at some large r_s , and hence changes the ground state symmetry. The existence of degrees of freedom related to spin and momentum makes it natural to consider the possibility of a magnetic instability or an instability that is related to the dispersion of a quasiparticle, which we call "dispersion instability" for short. There has been considerable previous theoretical work on the magnetic instability or spontaneous spin polarization of electron systems in zero magnetic field^{19,20,21,22,23,24,25,26,27,28,29,30,31,32,33,34,35,36}. For the dispersion instability, there has been theoretical work predicting the quasiparticle effective mass divergence^{37,38}. Many experiments^{1,2,3,4,5,6,7,8,9,10,11,12,13} have reported strongly enhanced magnetic susceptibility and effective mass¹⁴, but no real instability or divergence has been observed.

In spite of a great deal of past theoretical work investigating the magnetic instability possibilities in both 2D and 3D electron systems using a large variety of different theoretical techniques, a unified theoretical treatment of the ferromagnetic instability, starting from the weak-coupling Fermi liquid ground state with interaction

effects introduced systematically, is still lacking. For example, although there are many theoretical predictions in the literature for the interaction-driven divergence of the electronic spin susceptibility, the Landau g -factor, and the quasiparticle effective mass, the relationships among these transitions (or which one precedes the others, etc.) have not been studied within a unified theoretical prescription. In addition, the interacting spin susceptibility χ^* can be written as $\chi^* = g^* m^*$, where $m^*(g^*)$ are the effective mass (g -factor) of the system (with $\chi = gm$ denoting the corresponding bare quantities for the Fermi gas, and therefore an instability in the susceptibility χ^* could be caused by an instability in g^* or m^* (or both)). This issue has not been addressed in any detail in the existing theoretical literature. An important related question is the order of any possible ferromagnetic instability. It could be a second-order transition (the so-called Stoner instability) caused by the continuous divergence of the susceptibility as the critical density or r_s -value is approached from the weak-coupling side. Or it could be a first-order transition (the so-called Bloch ferromagnetism) which could happen abruptly at a specific r_s -value. Both have been predicted and studied in the literature, but their inter-relationship has not been clarified. In this paper we provide a comprehensive picture of the ferromagnetic instability in electron systems.

In this paper we examine the magnetic and dispersion properties of the 2D and 3D electron system using the so-called Random Phase Approximation (RPA)³⁹ within Fermi liquid theory. We assume the qualitative validity of RPA in studying the low-density electron system, which is argued in great detail in our previous work^{37,38,40}. Our key finding is that as the electron density of 2D or 3D electron liquid decreases, the system could develop a ferromagnetic instability of either Bloch type (characterized by the lowering of the spin-polarized ferromagnetic ground state energy below the spin-unpolarized paramagnetic ground state energy) or Stoner type (characterized by the divergence of magnetic susceptibility), and experience a first or second order quantum phase transition into a ferromagnetic liquid. And as the electron density further decreases, a new dispersion instability^{37,38} sets in, which is distinct from the ferromagnetic transition. We discuss the theoretical as well as experimental implications of the ferromagnetic instability at low electron densities.

The rest of this paper is organized as follows: in II we discuss briefly the background for Bloch and Stoner ferromagnetism in interacting electron liquids; in III we describe our basic RPA theoretical formalism involving ring or bubble diagrams and the Landau Fermi liquid theory; in IV we describe and discuss our theoretical results for ferromagnetic instability (at $T = 0$) as a function of density (i.e. the r_s parameter) in interacting 2D and 3D quantum Coulomb systems; we conclude in V with a discussion of possible experimental implications and many open questions.

II. BACKGROUND

The possibility of a density driven ferromagnetic transition in an interacting electron system was first suggested by Bloch⁴¹ more than 75 years ago. Bloch's basic idea, essentially a Hartree-Fock mean field theory, remains fundamentally valid even today. The idea is that at high density the electron system would be paramagnetic in order to optimize the kinetic energy cost (which is high in a high-density quantum fermionic system) whereas at low density the system should spontaneously spin-polarize itself into a ferromagnetic ground state in order to optimize the exchange energy arising from the Pauli principle and Coulomb interaction. This competition between kinetic energy (preferring paramagnetism) and exchange energy (preferring ferromagnetism) is at the heart of all current microscopic theories of itinerant (i.e. metallic) ferromagnetism through an energetic calculation (and comparison) for paramagnetic and ferromagnetic ground states in realistic systems is extremely hard. The fact that 'narrow band' metallic systems tend to be ferromagnetic is due to the constrained kinetic energy in these systems. For an electron gas (in a positive jellium background) it is a straightforward textbook exercise to write down the total Hartree-Fock energy per-particle as a sum of the non-interacting kinetic energy and the (Fock) exchange energy due to unscreened Coulomb interaction at $T = 0$ as

$$\begin{aligned} \frac{E}{N} &= E_{KE} + E_{ex} \\ &= \frac{0.55}{r_s^2} \left[(1 + \zeta)^{5/3} + (1 - \zeta)^{5/3} \right] \\ &\quad - \frac{0.23}{r_s} \left[(1 + \zeta)^{4/3} + (1 - \zeta)^{4/3} \right] \end{aligned} \quad (1)$$

for 3D system, and

$$\begin{aligned} \frac{E}{N} &= \frac{0.50}{r_s^2} (1 + \zeta)^2 \\ &\quad - \frac{0.30}{r_s} \left[(1 + \zeta)^{3/2} + (1 - \zeta)^{3/2} \right] \end{aligned} \quad (2)$$

for 2D systems, where $N = N_\uparrow + N_\downarrow$ is the total number density of electrons; $\zeta = (N_\uparrow - N_\downarrow)/N$ is their spin-polarization (or magnetism) density; $a_B^3 N = (\frac{4}{3}\pi r_s^3)^{-1}$ and $a_B^2 N = (\pi r_s^2)^{-1}$ define the dimensionless interaction parameters r_s in 2D and 3D respectively (with $a_B = \hbar^2/(me^2)$, the Bohr radius); and the energy is measured in Rydberg units (i.e. e^2/a_B). The first (second) term in each equation gives the kinetic (exchange) energy. Note that $\zeta = 1(0)$ denotes the ferromagnetic (paramagnetic) state. It is easy to see that the above Hartree-Fock energy expressions lead to a first-order ferromagnetic transition (the "Bloch ferromagnetism") at $r_s = r_B$ where $r_B \simeq 5.45$ (3D) and $r_B \simeq 2$ (2D), i.e. $E(\zeta = 1)$ ferromagnetic state is lower (higher) in energy than $E(\zeta = 0)$ paramagnetic state for $r_s > (<)r_B$. We refer to such energy-difference-driven abrupt (first order)

transition as Bloch ferromagnetism in the rest of this paper.

The Stoner ferromagnetic instability⁴² refers to the divergence of the spin susceptibility approaching a critical coupling constant $r_s = r_{St}$, from the paramagnetic ($r_s < r_{St}$) weak-coupling side. Such a divergent electronic spin susceptibility as a function of r_s indicates the onset of a second-order ferromagnetic transition at $r_s = r_{St}$ with the system being a paramagnetic for $r_s < r_{St}$ and a ferromagnetic for $r_s \geq r_{St}$ through a continuous magnetic phase transition. The simplest model to consider is, following Stoner's original work, a zero-range delta-function like interaction of strength ' I ' (a constant in momentum space) between the electrons, leading to an interacting static long-wavelength spin susceptibility (in the dynamical Hartree-Fock approximation) given by

$$\chi^*/\chi = (1 - D_0 I)^{-1},$$

where $D_0 \equiv D(E_F)$ is the electronic density of states at the Fermi energy. This immediately leads to the Stoner criterion for ferromagnetic instability defined by a divergent χ^*/χ when $1 - D_0 I = 0$. Since the 2D density of states is a density-independent constant, this instability criterion does not lead to a meaningful condition in 2D unless we arbitrarily define I to be the Coulomb interaction strength at Fermi wavelength at Fermi wavevector, whence the Stoner instability criterion leads to unphysically low r_s values for the ferromagnetic instability given by $r_{St} \simeq 0.7$ (2D) and $r_{St} \simeq 1.5$ (3D), which are absurdly small r_s -values and are unrealistic. Of course, in real electron systems the electron-electron interaction is the long-range Coulomb interaction, and therefore the simple Stoner instability criterion, defined by $D_0 I = 1$ where I is an effective short-range interaction strength, is inapplicable. But the basic idea of the ferromagnetic Stoner instability, defined by a continuous divergence of $\chi^*(r_s)$ as r_s is increased, still applied. We refer to the ferromagnetic transition defined or characterized by a divergence of the interacting susceptibility as the Stoner instability.

Our consideration for Bloch and Stoner ferromagnetic instabilities in electron liquids have necessarily been elementary in this section because we are just providing the background and defining the terminology in this section. In real electron liquids, the exchange-only Hartree-Fock approximation considered above for the Bloch instability is inadequate because correlation effects (i.e. energy contributions beyond Hartree-Fock) are known to be extremely important, and must be included in the energetic considerations. Similarly, the interacting susceptibility must be calculated for the real Coulomb interaction in the system, *not* for a hypothetical zero-range interaction, in order to obtain a better estimate of the Stoner instability criterion.

In the rest of this paper we consider both Bloch and Stoner ferromagnetic instabilities using better many-body approximations for Coulomb electron liquids. In particular, we use the many-body RPA (or equivalently,

the ring-diagram-approximation) theory to investigate both Bloch and Stoner ferromagnetic instabilities. In addition, we investigate the effective mass divergence of the interacting electron system on the same footing using the RPA self-energy calculation. Since, by definition, $\chi^* = g^* m^*$ (and $\chi = gm$), the various instabilities in χ^* and m^* allows us to sort out instabilities both the g -factor (i.e. ferromagnetic instabilities) and in the effective mass (i.e. dispersion instability). The quasiparticle effective mass instability in 2D and 3D systems has recently been discussed by us in details^{37,38}, and here we include results only for the sake of comparison without giving the details. It is important to emphasize that our many-body approximation does not involve any high-density or r_s -expansion, and RPA remains qualitatively valid for "metallic" ($r_s \approx 1 - 10$) densities, although its precise quantitative validity is hard to assess in the $r_s \gg 1$ regime. (RPA is exact in the $r_s \rightarrow 0$ limit, but this is *not* a particularly relevant point in discussing the ferromagnetic instabilities which occurs for $r_s > 1$.) An excellent early survey of metallic ferromagnetism (restricted entirely to 3D electron systems) can be found in the classic book by Herring⁴³.

III. THEORY

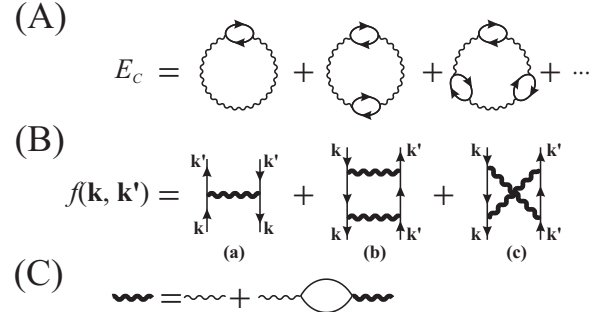


FIG. 1: The RPA Feynman diagram for: (A) the Coulomb interaction contribution to the ground state energy; (B) Landau's interaction function; (C) Dynamically screened interaction. The circles are polarization bubbles, the thin wiggly lines are the bare Coulomb interaction, and the solid lines the noninteracting electron Green's function.

In this work we follow the notation of Refs. 37,38,40. Within RPA^{37,38,39,40,44,45,46}, the Coulomb contribution to the ground state energy of a jellium electron system with long-range Coulomb interaction can be denoted by the Feynman diagrams shown in Fig. 1A. The quasi-particle energy is then obtained by $E_{\mathbf{k}} = \delta E_G / \delta n_{\mathbf{k}}$, where $n_{\mathbf{k}}$ is the distribution function at momentum \mathbf{k} . The second order derivative of the total ground state energy is referred to as Landau's interaction function: $f(\mathbf{k}, \mathbf{k}') = \delta^2 E_G / \delta n_{\mathbf{k}} \delta n_{\mathbf{k}'}$, represented by the Feynman diagram shown in Fig. 1B. Graphically, taking the $n_{\mathbf{k}}$ variational derivative of a quantity simply means that

one cuts one solid line of the Feynman diagram and takes the external momentum and frequency to be on-shell (i.e. $\omega = \mathbf{k}^2/2m - E_F$ with m the band electron mass and E_F the Fermi energy). We emphasize that the RPA as shown in Fig. 1 necessarily implies that the on-shell self-energy approximation is used for calculating the quasi-particle energy dispersion $E_{\mathbf{k}}$ and Landau's interaction function $f(\mathbf{k}, \mathbf{k}')$ since all energy and momenta in Fig. 1 correspond to the noninteracting system. Thus RPA self-energy approximation necessarily implies an on-shell approximation (Fig. 1A) as emphasized by Rice⁴⁴ a long time ago.

Following Hubbard's notation⁴⁵, the ground state energy per particle E_G/N with N the particle number can be written as $E_G/N = E_K/N - v(0)/2 + E_C/N$, where E_K is the kinetic energy, $v(0) = \int v_q d^d q / (2\pi)^d$ is the interaction energy at zero separation with the bare Coulomb interaction $v_q = 2\pi e^2/q$ for 2D and $v_q = 4\pi e^2/q^2$ for 3D, and E_C is the Coulomb contribution to the ground state energy (both exchange and correlation) which can be denoted as in Fig. 1A. Note that the singularities in $v(0)/2$ and E_C/N cancel out with each other. In the 2D system, it is easy to show⁴⁵ that RPA leads to

$$\frac{E_G}{N} = \frac{E_F}{2} + \frac{E_{ex}}{N} + \frac{16E_F}{g_s\pi} \int_0^\infty x dx \int du [\ln \epsilon(x, u) - \epsilon(x, u)], \quad (3)$$

where $\epsilon(q, \omega)$ is the dynamical dielectric function, g_s is the spin degeneracy ($g_s = 2$ for paramagnetic states and $g_s = 1$ for fully spin-polarized state), E_{ex} is the exchange part of the ground state energy. Note that in Eq. (3) we subtracted a term $\epsilon(q, \omega)$ from $\ln[\epsilon(q, \omega)]$ in order to handle the ultraviolet divergence in the integration. Similarly for 3D we have

$$\frac{E_G}{N} = \frac{3}{5}E_F + \frac{E_{ex}}{N} + \frac{48E_F}{g_s\pi} \int_0^\infty x^2 dx \int du [\ln \epsilon(x, u) - \epsilon(x, u)]. \quad (4)$$

It is convenient to convert all the expressions in terms of the dimensionless units r_s . The definition of r_s is as $r_s = 1/(\alpha k_F a_B)$ where k_F is the Fermi momentum and $a_B = 1/(me^2)$ is the Bohr radius. In 2D $\alpha = \sqrt{g_s}/2$ and in 3D $\alpha = (2g_s/9\pi)^{1/3}$. Also we choose $\hbar = 1$ throughout, which makes wavevector and momentum (as well as energy and frequency) equivalent. In these notations, it is easy to show that $E_{ex}/N = -8\alpha r_s/(3\pi)E_F$ for 2D, and $E_{ex}/N = -3\alpha r_s/(2\pi)E_F$ for 3D. In the actual calculation, the integration in Eqs. (3) and (4) can be performed on either real or imaginary axis. By examining the r_s and g_s dependence of the ground state energy, we study the Bloch magnetic instability of the electron system. The integrals in Eqs. (3) and (4) are the correlation contributions not included in our Hartree-Fock considerations of Bloch ferromagnetic in Sec. II. Note that $g_s = 1(2)$ corresponds to $\zeta = 1(0)$ in Sec. II.

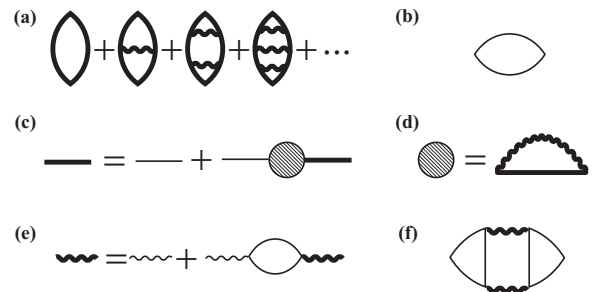


FIG. 2: (a) The ladder-bubble series for the interacting susceptibility with the bold straight line the interacting Green's function and the bold wavy line the dynamically screened interaction; (b) the noninteracting susceptibility; (c) the Dyson's equation for the interacting Green's function in terms of the noninteracting Green's function and the self-energy; (d) the self-energy in the leading-order expansion in the dynamical screening; (e) the Dyson's equation for the dynamically screened interaction in terms of the bare Coulomb interaction (thin wavy lines) and the polarization bubble; (f) a charge fluctuation diagram which does not contribute to spin susceptibility.

We investigate the Stoner instability by calculating the magnetic susceptibility χ^* within RPA which is represented by the Feynman diagram showed in Fig. 2. Direct calculation of these diagrams turns out to be difficult for the long ranged Coulomb interaction. However, at $T = 0$, Landau showed that χ^* can be equivalently expressed as the following equation⁴⁴:

$$\frac{\chi}{\chi^*} = \frac{m}{m^*} + \varpi \int f_e(\theta) \cos \theta d\theta, \quad (5)$$

where χ is the Pauli spin susceptibility, $f_e(\theta) = f_e(\mathbf{k}, \mathbf{k}')$ with \mathbf{k} and \mathbf{k}' on-shell; $\mathbf{k}^2/2m = \mathbf{k}'^2/2m (= E_F)$ is the exchange Landau's interaction function, θ is the angle between \mathbf{k} and \mathbf{k}' , $d\theta$ the element of solid angle along \mathbf{k}' in 3D and $d\theta$ in 2D, and $\varpi = 1/(2\pi)^2$ in 2D and $\varpi = k_F/(2\pi)^3$ in 3D. Similarly, the Landau theory expression for the effective mass m^* is⁴⁴

$$\frac{m}{m^*} = 1 - \varpi \int f(\theta) \cos \theta d\theta. \quad (6)$$

In Eq. (5), $f_e(\theta)$ is the exchange part of the Landau's interaction function, which is represented by Fig. 1B(a). This spin independent term is responsible for the difference between the ratio χ/χ^* and m/m^* ⁴⁴.

After we convert all the expressions in terms of the dimensionless parameter r_s , and use $2k_F$, $4E_F$, $2m$ as the momentum, energy, and mass units, we obtain the expression for the 2D magnetic susceptibility as

$$\frac{\chi}{\chi^*} = -\frac{2\alpha r_s}{\pi} + \frac{\sqrt{2}\alpha r_s}{\pi} \int_0^\infty x^2 dx \int_0^\infty du \left[\frac{1}{\epsilon(x, iu)} - 1 \right] \times \left[A\sqrt{1+A/R} - B\sqrt{1-A/R} \right] R^{-5/2}, \quad (7)$$

where $A = x^4 - x^2 - u$, $B = 2xu$, $R = \sqrt{A^2 + B^2}$. Similarly for 3D we have

$$\frac{\chi}{\chi^*} = -\frac{\alpha r_s}{\pi} + \frac{\alpha r_s}{2\pi^2} \int_0^\infty dx \int_0^\infty du \left[\frac{1}{\epsilon(x, iu)} - 1 \right] \times [\ln(F/G) - 2C/F + 2D/G], \quad (8)$$

where $C = 1 - q$, $D = 1 + q$, $F = C^2 + u^2$, $G = D^2 + u^2$. Note that in the expressions of the dielectric function $\epsilon(x, u)$, $x = q/(2k_F)$ and $u = \omega/(4E_F)$.

IV. RESULTS

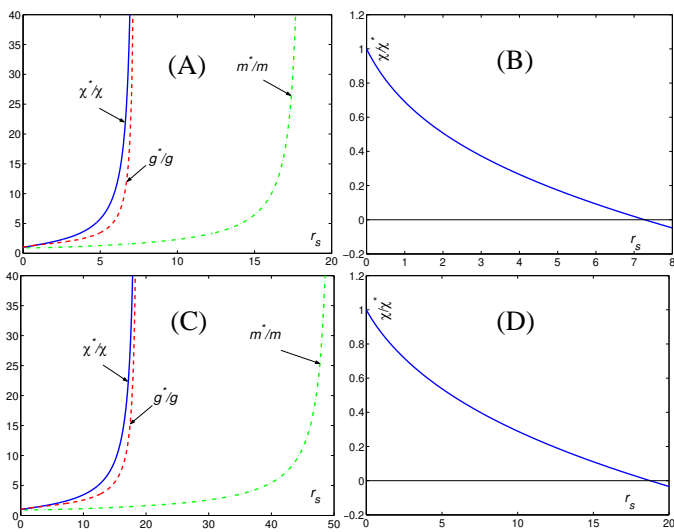


FIG. 3: (A) and (C): Calculated renormalized spin susceptibility χ^*/χ , effective mass m^*/m and g -factor g^*/g . For 2D system, χ^* and g^* diverge at $r_s \sim 7.3$ while m^* diverges at $r_s \sim 18.1$. For 3D system, χ^* and g^* diverges at $r_s \sim 18.7$ while m^* diverges at $r_s \sim 49.9$. (B) and (D): inverse susceptibility shows χ^* diverges at $r_s \sim 7.3$ for 2D and 18.7 for 3D systems. Note that the χ^* and g^* are calculated for paramagnetic systems ($g_s = 2$) while m^* are for ferromagnetic systems ($g_s = 1$).

In Fig. 3 we present the calculated magnetic susceptibility as a function of r_s for both 2D and 3D systems, together with the calculated g -factor $g^* = \chi^*/m^*$ and the effective mass m^* . It is clear from Fig. 3 that both 2D and 3D systems experience Stoner ferromagnetic instabilities, characterized by the divergence of magnetic susceptibility as the density decreases. It is important to note that this Stoner instability (i.e. divergence of χ^*) does not arise from an effective mass divergence since the m^* divergence happens at much lower densities. In other words, g^* and m^* both diverge, with the divergence of g^* occurring at a lower r_s value. For the 2D system, χ^* and g^* diverges at $r_s \sim 7.3$ while m^* diverges at $r_s \sim 18.1$. For the 3D system, χ^* and g^* diverge at $r_s \sim 18.7$ while m^* diverges at $r_s \sim 49.9$.

We emphasize that both m^* and g^* divergences actually happen independently and are completely unrelated phenomena. On the other hand, it is also worth mentioning that the g^* divergence does have some quantitative effect on the m^* divergence. After g^* diverges, the system becomes a ferromagnetic liquid, and the momentum distribution is different and the Fermi energy increases. This change results in a small increase in the critical r_s value where m^* diverges. In fact for $g_s = 2$ paramagnetic systems, m^* diverges at 16.1 for 2D and 47.8 for 3D³⁷, in contrast to $g_s = 1$ case where m^* diverges at 18.1 for 2D and 49.9 for 3D. But this effect is rather small and is of no particular significance.

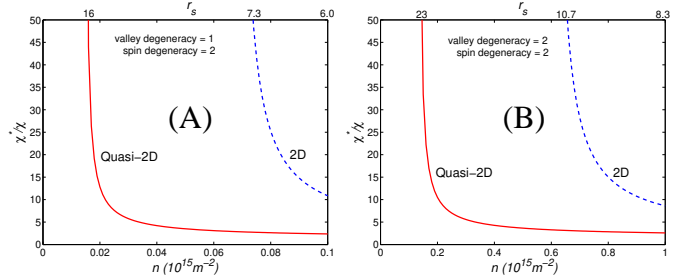


FIG. 4: Quasi-2D effects on magnetic susceptibility divergence. (A): GaAs quantum well system. (B): Si-inversion layer.

In real experimental systems, the value of r_s at which χ^* diverges should be influenced by many factors (even within our RPA many-body approximation scheme). Here we consider the valley degeneracy g_v and the finite width effect on the magnetic susceptibility divergence in semiconductor-based realistic 2D electron systems. The effect of g_v is exactly the same as the effect of g_s on the system, and therefore can be easily incorporated. For the finite width effect, we introduce a form factor to the Coulomb interaction, following the standard procedure described in detail in Refs. 47,48. Using appropriate semiconductor parameters, we obtain the susceptibility in GaAs quantum wells and Si-inversion layers, plotted in Fig. 4. It is clear from Fig. 4 that multi-valley degeneracy and finite width both suppress the divergence of the susceptibility renormalization, and make the critical r_s value for χ^* divergence considerably larger than the strict 2D results.

The magnetic susceptibility is a thermodynamic Fermi-surface property. As mentioned before, another way of studying the magnetic instability is to compare the ground state energy of the system for polarized and unpolarized states at different electron densities. This is the Bloch ferromagnetism discussed in Sec. II. Our results (Fig. 5) of RPA ground state energy for fully polarized and non-polarized electron states (using Eqs. (3) and (4)) in both 2D and 3D electron systems show similar characteristic. When r_s is very small (or electron densities high), both systems prefer non-polarized states. As r_s increases to a certain critical value ($r_s \sim 5.5$ for 2D and

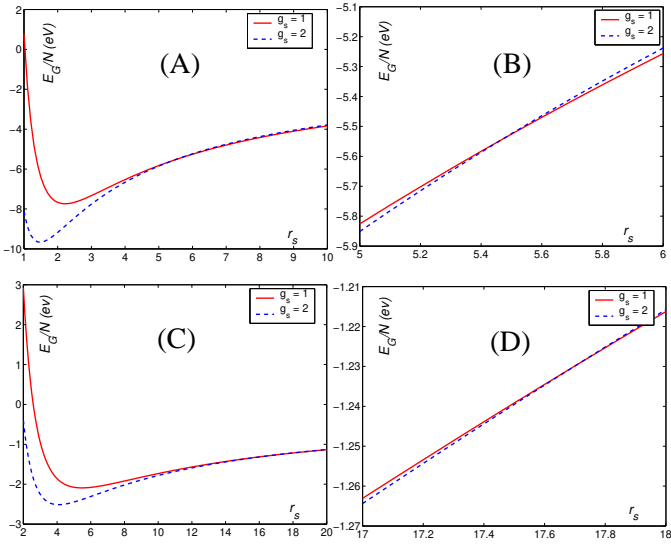


FIG. 5: (A) and (C): the RPA ground state energy per particle for polarized ($g_s = 1$) unpolarized ($g_s = 2$) cases as a function of r_s for 2D and 3D systems, calculated using Eq. (3) and Eq. (4). (B) and (D): details around the magnetic instability at $r_s \sim 5.5$ for 2D and 17.8 for 3D systems.

$r_s \sim 17.8$ for 3D) the ground state energy for the fully polarized electron state actually becomes lower than the non-polarized states. This clearly indicates that the system undergoes a Bloch type ferromagnetic instability due to the Coulomb electron-electron interaction in a low density 2D electron systems. Note that the critical r_s for the Bloch instability is substantially higher in the RPA theory (increasing from 2 to 5.5 in 2D and 5.45 to 17.8 in 3D) than in the Hartree Fock theory due to the inclusion of correlation energy.

Comparing Figs. 3 and 5 we conclude that, at least within our well-defined RPA ring-diagram many-body approximation scheme, the sequence of instabilities (as density decreases) the theory predicts for both 2D and 3D electron liquids is the following: Bloch ferromagnetism (i.e. an abrupt first order magnetic transition) at $r_s = 5.5$ (2D); 17.8 (3D); Stoner ferromagnetism characterized by a continuous divergence (i.e. a second order magnetic transition) of the interacting g -factor and of the susceptibility at $r_s = 7.3$ (2D), 18.7 (3D); the dispersion instability associated with the continuous divergence of the quasiparticle effective mass at $r_s = 18.1$ (2D), 49.9 (3D). Of course, comparing first and second order transitions is not particularly meaningful since their origins are fundamentally different, and a first order transition may always preempt a second order transition as seems to happen in Coulomb electron liquids with Bloch ferromagnetism always happening (both in 2D and 3D) at a slightly lower r_s values (5.5 versus 7.3 in 2D, and 17.8 versus 18.7 in 3D) although the difference in the critical r_s values for the two transitions (less than 10% in 3D and about 25% in 2D) is sufficiently small so that both Bloch and Stoner ferromagnetism remain of experimental

interest.

We also note that, by definition, $\chi^* \equiv g^*m^*$ (and $\chi = gm$), and therefore the divergence of the interacting susceptibility could be caused either by a divergence g -factor or a diverging effective mass. This issue has been much discussed and debated^{1,2,3,10,11,12,13} in the recent experimental literature on 2D semiconductor-based electron systems, where low-density divergence of both 2D susceptibility and effective mass has been reported. All we can say is that our theoretical results are only consistent with the susceptibility divergence as arising from the divergence of the interacting g -factor, not the effective mass, since the g -factor divergence occurs at much lower r_s -values, $r_s \sim 7.3$ (18.7) in 2D (3D) for g^*/g divergence versus $r_s \sim 18.1$ (49.9) in 2D (3D) for m^*/m divergence. We add that in realistic quasi-2D semiconductor system (our Fig. 4) the susceptibility (as well as effective mass) divergence occurs at substantially higher r_s values due to the considerable softening of the Coulomb interaction from its strict 2D form due to the finite-width effect.

V. DISCUSSION

Both Bloch and Stoner instabilities imply that 2D and 3D electron systems interacting via the long range Coulomb interaction undergo a $T = 0$ ferromagnetic quantum phase transition from a high-density paramagnetic state to a low-density ferromagnetic state either through a first order (Bloch) transition or a second-order (Stoner) transition (with a continuous divergent susceptibility) at a critical r_s -value. Given that the critical r_s value(s) for the transition(s) we obtain within our RPA many-body theory is rather large (i.e. $r_s \gg 1$), we do not expect our predicted r_s parameter for ferromagnetic transitions in 2D and 3D electron systems to be reliable. But the basic trends, such as the sequence of instabilities (i.e. Bloch followed by Stoner followed by the dispersion instability with diverging mass as the density is lowered) or the suppression of the transition to much lower densities in *quasi*-2D systems, should be valid, in general. Indeed quantum phase transitions predicted by RPA (or for that matter even by the simpler Hartree-Fock approximation) are always found to occur in the numerical quantum Monte Carlo (QMC) simulation albeit at higher r_s values. This is certainly true for electron liquid ferromagnetic instabilities. QMC simulations predict 2D (3D) ferromagnetic instability to occur around $r_s \sim 25 - 30$ (50 - 60). It is, however, difficult to ascertain the order of the ferromagnetic transition in QMC numerical simulations – our RPA theory predicts the first-order Bloch instability to occur first as the density is being lowered.

Much has been written about the validity of the RPA many-body approximation at low carrier densities ($r_s > 1$). We have little to add to this issue beyond the detailed discussion we already provided in our recent publications^{37,40}. We want to emphasize that, although RPA is exact in the $r_s \rightarrow 0$ limit, it is by no means a theory

based on an r_s expansion – it is a self-consistent field theory based on an expansion in the dynamically screened interaction which should be qualitatively valid for *all* r_s below the Wigner crystallization of the electron liquid. In fact, RPA is found to be quantitatively valid in 3D systems⁴⁴ at metallic densities ($r_s \sim 3 - 6$) and in 2D systems for r_s up to 10 – 15 where comparison with experiment has been carried out⁴⁹. Often the error in the calculation arising from other effects (e.g. finite temperature⁵⁰, finite quasi-2D width, band structure, etc.) turn out to be larger than that included in the RPA approximation, and therefore improvement beyond RPA (short of a full-fledged QMC calculation) becomes meaningless.

One can try to “improve” upon RPA by including local field corrections to the dynamical electron polarizability (i.e. bare bubble of RPA) which, in some crude manner, simulates the incorporation of higher-order vertex corrections in the theory. But such local field corrections are uncontrolled, and probably inconsistent, since many diagrams in the same order are typically left out. We are therefore unconvinced that the inclusion of local field corrections in the theory is necessarily an improvement on RPA. The great conceptual advantage of RPA is that it is a well-defined approximation that is both highly physically motivated (i.e. dynamical screening) and theoretically exact in the high-density ($r_s \rightarrow 0$) limit. Attempted improvement upon RPA through the arbitrary inclusion of local field correction may neither be theoretically justifiable nor more reliable. Keeping these caveats in mind we have carried out our exchange instability calculations using the Hubbard local field corrections⁴⁵, and we find no qualitative changes from the RPA results presented in this paper. The critical r_s values for the occurrence of the ferromagnetic instability change somewhat in the presence of the local field correction, but this is a result without any significance since the precise values of critical r_s are expected to be not particularly accurate in any of these theories. The fact that the basic qualitative conclusions about the various instabilities do not change in the presence of local field corrections demonstrate the qualitative robustness of our RPA-based results.

In discussing possible experimental implications of our results, we note the great recent experimental interest in the literature on the possibility of a density-driven ferromagnetic transition in semiconductor-based 2D carrier systems where very low carrier densities ($r_s \lesssim 10$) can be achieved in rather high-quality samples^{1,2,3,4,5,6,7,8,9,10,11,12,13,14}. There are recent experimental claims^{1,2,3,12} of the observation of a low density susceptibility divergence in Si MOSFETs for $r_s \sim 7 - 10$. Although the experimental susceptibility behavior as a function of density (or, r_s) looks similar to our theoretical results in Figs. 3 and 4, we are skeptical about the significance of this agreement. There are several reasons for our skepticism. First, the experimental claimed susceptibility divergence occurs at far too high a density ($r_s \sim 7$) compared with the theory where we find the RPA susceptibility divergence in realistic Si MOSFETs

(Fig. 4) to be occurring at $r_s \approx 23$. This RPA predictions for critical r_s (~ 23) is most likely the lower bound – any real susceptibility divergence is expected to occur at higher r_s values ($r_s > 23$). Second, the experimental divergence of $\chi^*/\chi \equiv g^*m^*/gm$ has been claimed^{1,2,3} to be arising from an effective mass divergence, *not* the g -factor divergence as we find in our theory. Our theoretical effective mass divergence, in fact, occurs at a critical r_s more than twice as large as the corresponding χ^* critical r_s . In fact, our *quasi*-2D effective mass divergence^{37,38} occurs for $r_s > 40$! Third, there has been no experimental evidence for the existence of a low-density ferromagnetic phase such as hysteresis, remanence, etc. If there is indeed a ferromagnetic transition, one should be able to observe ferromagnetic behavior at densities below the ferromagnetic critical density (i.e. for r_s values larger than the point of χ^* divergence). No such direct ferromagnetic behavior has ever been observed in a low-density 2D system casting serious doubts on the claims of the observation of a 2D ferromagnetic transition. A very recent extremely careful and detailed measurement of 2D susceptibility in a high-mobility n-GaAs system⁹ finds no divergence in χ^*/χ up to $r_s \approx 12$, calling into question the earlier claims of susceptibility divergence in Si MOSFETs at lower r_s values. In addition, a direct thermodynamic measurement⁴ of 2D susceptibility in Si MOSFETs also does not find a ferromagnetic instability. What is clear is the observed strong enhancement of χ^*/χ (and m^*/m) as a function of increasing r_s which is consistent with our theoretical findings. But the actual existence of a low-density electron liquid ferromagnetic transition has not be established experimentally in our opinion.

Finally we discuss some of the earlier literature that is of relevance to our work. Our calculation of the ground state energy for polarized and unpolarized states partially confirms the numerical results of Rajagopal *et. al.*⁵¹, who also considered the possibility of partially polarized states, and found that for certain range of electron densities, the system prefers a partially polarized ferromagnetic state in the 3D system. Similar results were also derived using the Quantum Monte Carlo method¹⁷. In this paper we neglect this possibility because our main purpose is to establish the relation between magnetic instabilities and dispersion instabilities, and the densities of the partial spin-polarization region are much higher than the density that corresponds to the divergence of effective mass. Partial spin-polarization does not occur in 2D systems, and thus this issue does not arise for our 2D calculations, which is the main focus of our work. For the magnetic susceptibility, there have been earlier RPA calculations in 2D^{30,31,32,52,53} and 3D²⁹, and QMC calculations in 2D¹⁸. Only Shastry²⁹ predicted a susceptibility divergence in 3D systems, and our results confirmed his conclusion. No previous work considered the inter relations, among Bloch instability, Stoner instability and dispersion instability. Our work is the only work in the literature connecting all these density-driven elec-

tron liquid instabilities within one coherent theoretical framework.

This work is supported by NSF, DARPA, ONR, LPS, and ARO.

¹ A. A. Shashkin, S. V. Kravchenko, V. T. Dolgopolov, and T. M. Klapwijk, Phys. Rev. B **66**, 073303 (2002).

² A. A. Shashkin, M. Rahimi, S. Anissimova, S. V. Kravchenko, V. T. Dolgopolov, and T. M. Klapwijk, Phys. Rev. Lett. **91**, 046403 (2003).

³ A. A. Shashkin, S. V. Kravchenko, V. T. Dolgopolov, and T. M. Klapwijk, Phys. Rev. Lett. **87**, 086801 (2001).

⁴ O. Prus, Y. Yaish, M. Reznikov, U. Sivan, and V. Pudalov, Phys. Rev. B **67**, 205407 (2003).

⁵ C. L. Chang, S. P. Shukla, W. Pan, V. Venkataraman, J. C. Sturm, and M. Shayegan, Thin Solid Films **321**, 51 (1998).

⁶ E. Tutuc, E. P. D. Poortere, S. J. Papadakis, and M. Shayegan, Phys. Rev. Lett. **86**, 2858 (2001).

⁷ E. Tutuc, S. Melinte, and M. Shayegan, Phys. Rev. Lett. **88**, 036805 (2002).

⁸ E. P. D. Poortere, E. Tutuc, Y. P. Shkolnikov, K. Vakili, and M. Shayegan, Phys. Rev. B **66**, 161308(R) (2002).

⁹ J. Zhu, H. L. Stormer, L. N. Pfeiffer, K. W. Baldwin, and K. W. West, Phys. Rev. Lett. **90**, 056805 (2003).

¹⁰ V. M. Pudalov et al., Phys. Rev. Lett. **89**, 219702 (2002).

¹¹ V. M. Pudalov, M. E. Gershenson, H. Kojima, G. Brunthaler, A. Prinz, and G. Bauer, Phys. Rev. Lett. **91**, 126403 (2003).

¹² S. A. Vitkalov, H. Zheng, K. M. Mertes, M. P. Sarachik, and T. M. Klapwijk, Phys. Rev. Lett. **87**, 086401 (2001); M. P. Sarachik and S. A. Vitkalov, cond-mat/0209113.

¹³ V. M. Pudalov, M. E. Gershenson, H. Kojima, N. Butch, E. M. Dzhur, G. Brunthaler, A. Prinz, and G. Bauer, Phys. Rev. Lett. **88**, 196404 (2002).

¹⁴ Y.-W. Tan, J. Zhu, H. L. Stormer, L. N. Pfeiffer, K. W. Baldwin, and K. W. West, cond-mat/0412260.

¹⁵ E. Wigner, Phys. Rev. **46**, 1002 (1934).

¹⁶ B. Tanatar and D. Ceperley, Phys. Rev. B **39**, 5005 (1989).

¹⁷ G. Ortiz, M. Harris, and P. Ballone, Phys. Rev. Lett. **82**, 5317 (1999).

¹⁸ C. Attaccalite, S. Moroni, P. Gori-Giorgi, and G. B. Bachelet, Phys. Rev. Lett. **88**, 256601 (2002).

¹⁹ M. F. Bishop and T. McMullen, Phys. Rev. B **62**, 15160 (2000).

²⁰ V. V'yurkov and A. Vetrov, Nanotechnology **11**, 336 (2000).

²¹ G. Benenti, G. Caldara, and D. L. Shepelyansky, Phys. Rev. Lett. **86**, 5333 (2001).

²² A. Ishihara and T. Toyoda, Phys. Rev. B **19**, 831 (1979).

²³ A. Ishihara and Y. Kojima, Phys. Rev. B **11**, 710 (1975).

²⁴ D. Y. Kojima and A. Ishihara, Phys. Rev. B **20**, 489 (1979).

²⁵ I. A. Shelykh, N. T. Bagraev, and L. E. Klyachkin, Semiconductors **37**, 1390 (2003).

²⁶ I. A. Shelykh, N. T. Bagraev, and L. E. Klyachkin, Phys. of the Solid State **45**, 2189 (2003).

²⁷ A. W. Overhauser, Phys. Rev. **128**, 1437 (1962).

²⁸ S. Misawa, Phys. Rev. **140**, A1645 (1965).

²⁹ B. S. Shastry, Phys. Rev. B **17**, 385 (1978).

³⁰ S. Yarlagadda and G. Giuliani, Phys. Rev. B **38**, 10966 (1988).

³¹ S. Yarlagadda and G. Giuliani, Phys. Rev. B **40**, 5432 (1989).

³² S. Yarlagadda and G. Giuliani, Phys. Rev. B **49**, 14188 (1994).

³³ J. Janak, Phys. Rev. **178**, 1416 (1969).

³⁴ S. Doniach and S. Engelsberg, Phys. Rev. Lett. **17**, 750 (1966).

³⁵ D. Coffey and K. S. Bedell, Phys. Rev. Lett. **71**, 1043 (1993).

³⁶ D. Coffey and C. J. Pethick, Phys. Rev. B **37**, 1647 (1988).

³⁷ Y. Zhang and S. Das Sarma, cond-mat/0312565; to appear in Phys. Rev. B .

³⁸ Y. Zhang, V. M. Yakovenko, and S. Das Sarma, cond-mat/0410039; to appear in Phys. Rev. B .

³⁹ A. A. Abrikosov, L. P. Gor'kov, and I. E. Dzyaloshinskii, *Methods of quantum field theory in statistical physics* (Dover Publications, New York, 1963); G. D. Mahan, *Many-Particle Physics* (Plenum Press, New York, 1981); A. L. Fetter and J. D. Walecka, *Quantum theory of many-particle systems* (McGraw-Hill, San Francisco, 1971).

⁴⁰ S. Das Sarma, V. M. Galitski, and Y. Zhang, Phys. Rev. B **69**, 125334 (2004); Ying Zhang and S. Das Sarma, Phys. Rev. B **70**, 035104 (2004).

⁴¹ F. Bloch, Z. Phys. **57**, 545 (1929).

⁴² E. C. Stoner, Proc. Roy. Soc. A **165**, 372 (1938); A **169**, 339 (1938).

⁴³ C. Herring, *Magnetism* (Academic Press, N.Y., 1966).

⁴⁴ T. M. Rice, Ann. Phys. (N. Y.) **31**, 100 (1965).

⁴⁵ J. Hubbard, Proc. Roy. Soc. **A240**, 539 (1957); **A243**, 336 (1957).

⁴⁶ L. Hedin, Phys. Rev. **139** (1965).

⁴⁷ T. Ando, A. B. Fowler, and F. Stern, Rev. Mod. Phys. **54**, 437 (1982).

⁴⁸ Y. Zhang and S. Das Sarma, cond-mat/0408335.

⁴⁹ E. H. Hwang and S. Das Sarma, Phys. Rev. B **64**, 165409 (2001).

⁵⁰ S. Das Sarma, V. M. Galitski, and Y. Zhang, Phys. Rev. B **69**, 125334 (2004); Y. Zhang and S. Das Sarma, Phys. Rev. B **70**, 035104 (2004); V. M. Galitski and S. Das Sarma, Phys. Rev. B **70**, 035111 (2004); A. V. Chubukov and D. L. Maslov, Phys. Rev. B **68**, 155113 (2003).

⁵¹ A. K. Rajagopal and J. C. Kimball, Phys. Rev. B **15**, 2819 (1977).

⁵² S. Yarlagadda and G. Giuliani, Phys. Rev. B **49**, 14172 (1994).

⁵³ G. E. Santoro and G. Giuliani, Phys. Rev. B **39**, 12818 (1989).